INTERNATIONAL JOURNAL OF AUTOMOTIVE AND MECHANICAL ENGINEERING
ISSN: 2229-8649 e-ISSN: 2180-1606
VOL. 21, ISSUE 1, 2024, 11064 – 11073
DOI: https://doi.org/10.15282/ijame.21.1.2024.10.0856

RESEARCH ARTICLE

Initial Study on Rheological Behaviour of Hydroxyapatites / Polylactic Acid Composite for 3D Printing Filament

Afeeqa Puteri Marzuki[1], Mohd Alfiqrie Mohd Nasir[1], Farrahshaida Mohd Salleh[1]*, Muhammad Hussain Ismail[1], Bibi Intan Suraya Murat[1], and Marzuki Ibrahim[2]

[1]College of Engineering, School of Mechanical Engineering, Universiti Teknologi MARA, 40450 Shah Alam, Selangor, Malaysia
[2]Centre of Design Studies, Faculty of Innovative Design and Technology, Universiti Sultan Zainal Abidin, Gong Badak Campus, 21300 Kuala Nerus, Terengganu, Malaysia

ABSTRACT - The present fused deposition modeling (FDM) printing process has concentrated on combining metal or ceramic filled with polymer because it could provide a strong composite in layered manufacturing technology in comparison to a single polymer material. However, the ability of the composite material to flow into the extruder becomes an obstacle because of the changes in the polymer concentration and dispersion of filler particles in producing the printed part. Hence, the rheological behavior of Hydroxyapatites (HAp) / Polylactic Acid (PLA) composite with different contents of HAp was studied to assess its ability to flow through the extruder during the 3D printing process. Measurements such as pycnometer density, thermal analysis (DSC) and FT-IR were performed on the composite feedstock containing a variation of 10% to 30% HAp powder. The feedstocks behavior then were characterized by rheological tests at three different temperatures (140 °C, 150 °C, and 160 °C). The composition of PLA/20HAp has produced optimum rheological behavior with effective flow behavior index (*n*) and activation energy (*E*) of 0.396 and 89.03 kJ/mol, respectively which is suitable for extruding out the HAp/PLA composite to become a 3D printing filament material.

ARTICLE HISTORY
Received : 20th June 2023
Revised : 25th Oct. 2023
Accepted : 23rd Jan. 2024
Published : 20th Mar. 2024

KEYWORDS
Polylactic acid
Hydroxyapatite
Rheological behaviour
Composite filament
3D printing

1.0 INTRODUCTION

Three-dimensional (3D) printing, known as additive manufacturing (AM), is a technology that allows the fabrication of an object by sequentially layering materials on top of one another. Currently, the most widely used AM technology is the fused deposition modeling (FDM) method, which works by melting the thermoplastic polymer filament and extruding it layer by layer through a nozzle to form a solid 3D printed part, as shown in Figure 1. In 3D printing, the common material for filament is made of thermoplastic materials such as polylactic acid (PLA), acrylonitrile butadiene styrene (ABS) and polycarbonate (PC). Their excellent material properties such as low melting point and flexibility to form various shapes make them a popular choice for 3D printing technology [1]. Over the years, the potential of 3D printing using only polymers has been expanded to other fields and applications, using other natural materials, metals, or combined materials to print specific or customized products. In recent years, developers have found ways to print composite materials that will improve the durability and structure of 3D-printed products. While the process of 3D printing composite materials is not in the mainstream yet, many researchers have started to investigate the potential of new material to become the filament for 3D printers and soon could replace the traditional way of fabricating tailored-made products such as in the medical, automotive, and aerospace industries. Through 3D printing technology, the products' internal porosity and interconnected structure can be well controlled.

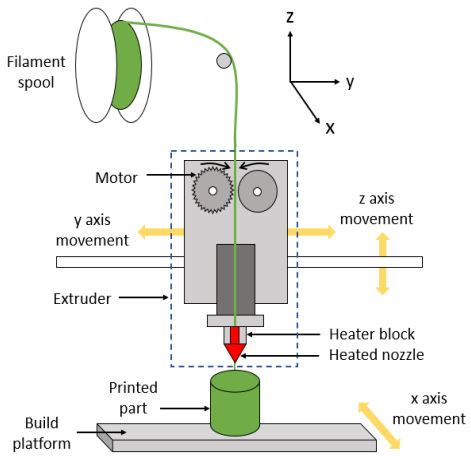

Figure 1. Schematic diagram of FDM [2]

*CORRESPONDING AUTHOR | Farrahshaida Mohd Salleh | ✉ fshaida@uitm.edu.my
© 2024 The Author(s). Published by Universiti Malaysia Pahang Al-Sultan Abdullah Publishing. This is an open access article under the CC BY-NC 4.0 International license

However, this 3D printing manufacturing technique relies on material availability in filament form, which is extruded through a heated nozzle, and deposited layer upon layer. For producing the filament, several factors need to be considered: material loading, binder ratio, rheological behavior, pressure and temperature setting. For material loading, a balanced mixture of powder and binder is required as it will define the success or failure of the extrusion process. Too little binder (more powder) leads to a high-viscosity feedstock, resulting in a porous (void) and brittle structure. Meanwhile, too little powder (more binder) leads to a feedstock inhomogeneity as the material becomes viscous which will produce defective products. Hence, before printing, the rheological behavior of the mixture should be characterized first to evaluate its flowability. This is to ensure that this mixture can achieve the optimum binder composition [3].

In this study, the rheological properties of composite feedstock are essential to fix the optimum process, and access materials flow behavior during processing because it reacts to processes that occur throughout the printing phases, such as viscoelastic behavior and viscous flow in the nozzle during interlayer welding [4]. In addition, the viscosity value in rheology is important to characterize the flow behavior of the materials [5]. Research in 2021 showed that the recommended range of viscosity for FDM 3D printing is between 10^2 and 10^5 Pa.s [6]. In 3D printing, lower viscosity is needed as the force of the flow will be minor to obtain a high printing quality [7].

Several recent reviews have been published for 3D printing in bone tissue engineering as this technology can directly print the bone with designated shape, interconnected structure and porosity. In bone tissue engineering, the material requirements for bone replacement are excellent bioactive properties and good mechanical strength like ceramic-based material. It has excellent bioactivity and biocompatibility characteristics in the in-vivo environment and is resistant to corrosion if compared with metallic and polymer-based [8]. In this study, poly-lactic acid (PLA) is a potential polymer that can be biodegraded and has a similar compressive modulus (3.5 GPa) to natural bone (1.15 to 5.44 GPa) [9]. However, the PLA has shown low biological activity and the idea of combining PLA with HAp seems to be a good option to increase biological activity and enhance bioresorbability [10]. HAp is widely used as a coating material to increase surface activity which is biocompatible with bone tissues due to its chemical composition that is closely identical to the mineral phase of bone. Senatov et al. [11] found that adding HAp into the PLA boosted the osseointegration and raised the recovery stress and strain of the PLA shape-memory particles for bone defects. However, the agglomeration of the ceramic particles could affect the flowability of the HAp/PLA composite feedstock during the extruding process, making it harder to pass through the printer nozzle.

Hence, this study aims to develop PLA-based polymer composite filaments containing synthetic HAp, for biomedical applications in FDM printers by investigating the rheological properties of HAp/PLA composite feedstock. Different content of HAp filler up to 30 wt% will be investigated as its influence on the interfacial bonding between PLA and HAp which affects the homogeneity, strength and functionality of the composites [12]–[14]. The feedstock will be investigated via a capillary rheometer for viscosity analysis as a function of temperatures and shear rates. The identification of the best feedstock formulation with an optimum rheological behavior is an important step toward producing biocomposite filaments for the 3D printing of implant bone.

2.0 MATERIAL AND METHODS

2.1 Raw Materials

PLA powder from Shenzhen Esun Industrial Co. Ltd (China) with an average particle size and density of 550 µm (30 mesh) and 1.272 ± 0.0014 g/cm^3, respectively, has been used in this study. Meanwhile, the HAp powder was purchased from Sigma Aldrich (04238, with purity ≥ 90%). Figure 2 shows the discrete particles of HAp powder with agglomeration flake shape under SEM observation. The particle size of the HAp powder was around 2.56 µm to 16.96 µm, measured by using a particle size analyzer (Malvern). The density for HAp powder was 2.984 ± 0.0034 g/cm^3.

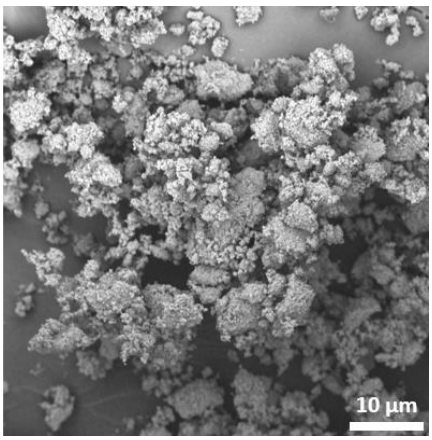

Figure 2. HAp powder under SEM image

2.2 Preparation of the HAp/PLA Feedstock

The composition ratio between HAp and PLA has been calculated using the composite volume fraction before proceeding with the mixing and blending process. HAp powder was then mixed and blended with PLA using a planetary mixer machine, by following the compositions as shown in Table 1. The temperature was set at 170 °C with a speed of 30 rpm [15]–[17]. Later, the homogeneity of the mixture for HAp/PLA will be evaluated by a helium pycnometer density. The theoretical density was calculated using the rule of the mixture as shown in Equation (1), where ρ is material density and v is volume fraction of material.

$$\rho_{composite} = v_{PLA} \cdot \rho_{PLA} + v_{HAp} \cdot \rho_{HAp} \quad (1)$$

Table 1. Mass composition of HAp/PLA

HAp (wt%)	PLA (wt%)	Name
0	100	PLA
10	90	PLA/10HAp
20	80	PLA/20HAp
30	70	PLA/30HAp

2.3 Characterization of HAp/PLA composite

Physical characterizations were conducted on the HAp/PLA composite for each composition. In order to determine the glass transition and melting temperature, the thermal stability of PLA was evaluated using differential scanning calorimetry (DSC) at a range of temperatures between 30 °C to 250 °C. The heating rate was constant at 10 °C min $^{-1}$ in a nitrogen atmosphere with a flow rate of 20 mL/min. Then, FTIR analysis was conducted to determine the functional groups in the neat and composite material using a Fourier transform infrared spectrometer (Spectrum One), wavelength 2000 cm^{-1} – 500 cm^{-1}. The rheological properties of the HAp/PLA composite were assessed at multiple temperatures (140 °C, 150 °C, and 160 °C) by using a Bohlin Instrument RH2000 capillary rheometer. A pressure of 70 MPa and a maximal shear rate of 1,000 s^{-1} were established on the capillary die, which has a diameter of 1 mm.

3.0 RESULTS AND DISCUSSIONS

3.1 Pycnometer density

The density analysis for PLA and HAp/PLA composite was obtained using the pycnometer principle that used helium as an analysis gas and the results were reported in Table 2Table 2.. In comparison with pure PLA, HAp/PLA composite has a higher density due to the addition of ceramic filler. This result obtained agreed with the previous studies where the density value for HAp/PLA composite of 5, 10, 15 and 25 wt% of HAp were 1.1, 1.5, 2.0, and 3.0 g/cm^3, respectively [18]. This indicates that the PLA composite density was affected by the presence of HAp in the composition as the ceramic density (2.984 g/cm^3) was greater than the PLA density (1.272 g/cm^3).

In 3D printing, this pycnometer density finding is significant in improving the print quality and structural integrity. This data ensures that the printed parts meet specific requirements and quality standards, especially in critical applications like medical implants where structural integrity and biocompatibility are essential. Variations in density may indicate the uneven distribution of the composite materials which affects the variations in mechanical properties. For instance, the regions with higher HAp concentration may be more brittle, while regions with lower HAp concentration may lack necessary reinforcement. Moreover, the print quality will be issued as the uneven dispersion can lead to inconsistencies in layer adhesion, print warping, or extrusion problems during the printing process. Hence, the compatibility assessment through density measurements is a vital step in ensuring the uniform distribution of materials in PLA/HAp composites. It helps identify areas where improvements are needed to achieve the desired properties and quality in printed parts, particularly in applications where consistency and structural integrity are of the utmost importance [19]–[21].

Table 2. Density result of HAp/PLA feedstocks at different compositions

Feedstock Composition	Density (g/cm^3)
PLA	1.272
PLA/10HAp	1.358
PLA/20HAp	1.410
PLA/30HAp	1.499

3.2 Thermal Analysis

The thermal analysis for all compositions of HAp/PLA composite was obtained by conducting a DSC test in the range of 30 °C - 250 °C to assess the effect of the HAp on the glass transition temperature, T_g and melting temperature, T_m towards PLA. Based on the results in Figure 3, the presence of the ceramic phase has no significant effect on the T_m of PLA even with the greatest HAp content. The melting peak displayed was in the range of 160 -180 °C, centered at about

166 -169 °C. Different melting peaks were reported by Backes et al. [22], Esposito Corcione et al. [12], and Senatov et al. [11] as T_m was influenced by the size and crystalline lamellae perfection that can develop on HAp particles as well as in the bulk of the polymer matrix. In contrast, the value of T_g had decreased drastically as shown in Table 3 where it can be related to the addition of HAp. These indicated that the presence of HAp in a polymer mixture had altered the intermolecular forces and chain dynamics, leading towards a reduction in the T_g [11]. For crystallization temperature, T_c, this thermal analysis only appeared at PLA/20HAp and had an absence for the other composition. The presence or absence of T_c in this particular composition might be due to the presence of the impurities, the processing conditions and the chemical structure, which can affect the ability of the material to crystallize [23].

Within the realm of 3D printing, the ability of the material to undergo crystallization or maintain an amorphous state can impact the overall printing efficiency and the occurrence of defects. The presence of T_c in PLA/20HAp indicates its crystalline behavior might enhance the mechanical properties of printed objects but it may also elevate the possibility of warping and shrinkage. However, utilizing materials that exhibit well-defined thermal properties can result in printing outcomes that are more predictable and controllable. In this case, thermal analysis findings assist in controlling and managing those factors which are impurities, processing conditions and chemical structure to minimize printing defects and improve the quality of printed objects [24], [25].

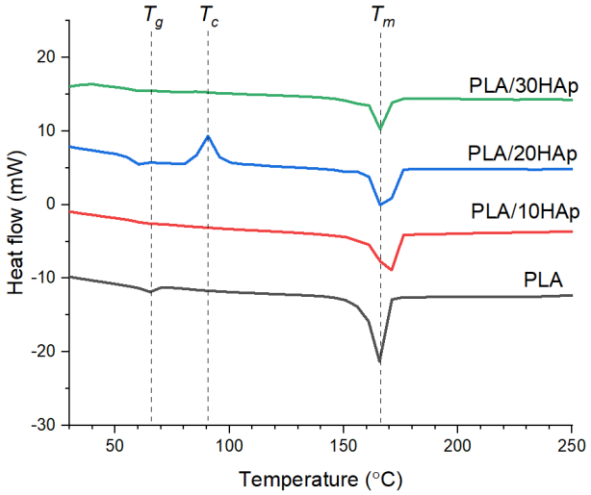

Figure 3. DSC curves for HAp/PLA composite with different HAp content

Table 3. DSC analysis for HAp/PLA composite with different HAp content

Feedstock Composition	T_g (°C)	T_m (°C)
PLA	65.95	166.88
PLA/10HAp	63.18	169.11
PLA/20HAp	57.99	167.60
PLA/30HAp	40.17	168.06

3.3 FT-IR

Figure 4 shows the FTIR spectrum of HAp/PLA composite with different content of HAp. The FTIR analysis was conducted to determine the functional groups in the material. For the HAp, carbonate group, PO_4^{3-} was identified at peaks of 565, 602, 962 and 1028 cm^{-1} in agreement with the previous studies where PO_4^{3-} peaks appeared at 564, 604, 962 and 1032 cm^{-1} [26]. As demonstrated in the FTIR spectrum for HAp/PLA composite, increasing the HAp content increased the peaks and intensity corresponding to the PO_4^{3-} characteristic absorption peak. These peaks indicate the existence of HAp in the composite. Moreover, for the PLA, groups of carbonyl and methyl which are expressed by chemical formulae of C=O and $-CH_3$ were clearly shown at peaks 1749 cm^{-1} and 1451 cm^{-1}, respectively. The peaks of the ether group, C-O-C also was observed at 1182 cm^{-1} and 1082 cm^{-1} [27]. Similar peaks also appeared in all HAp/PLA composites. This indicates that the findings validated the presence of HAp and PLA in the composites.

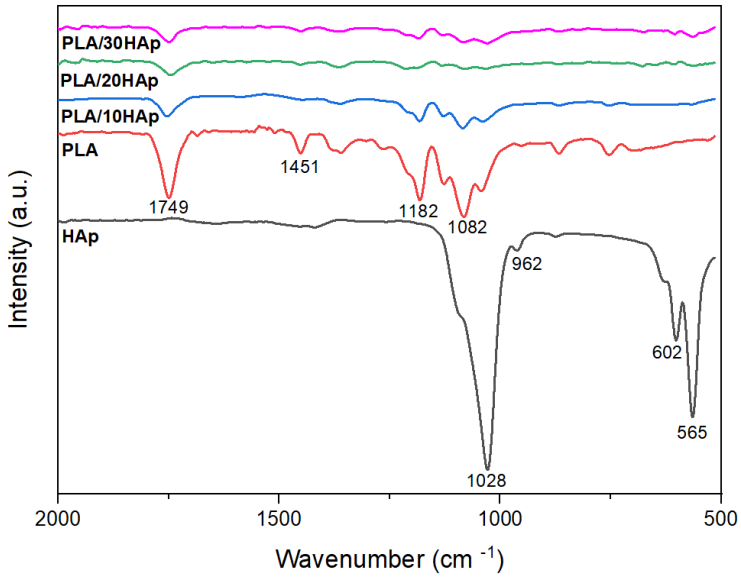

Figure 4. FTIR of HAp/PLA composite with different HAp content

3.4 Rheological Analysis

An initial study of the filament processability was conducted for the HAp/PLA composite by analyzing the rheological behavior of the HAp/PLA feedstock using a capillary rheometer. Additionally, precise control of the viscosity of HAp/PLA filament is essential as it will have an impact on printing accuracy. Figure 5 shows the rheological behavior of PLA and HAp/PLA composite with HAp content of 10, 20 and 30 wt% at three different temperatures, 140, 150 and 160 °C.

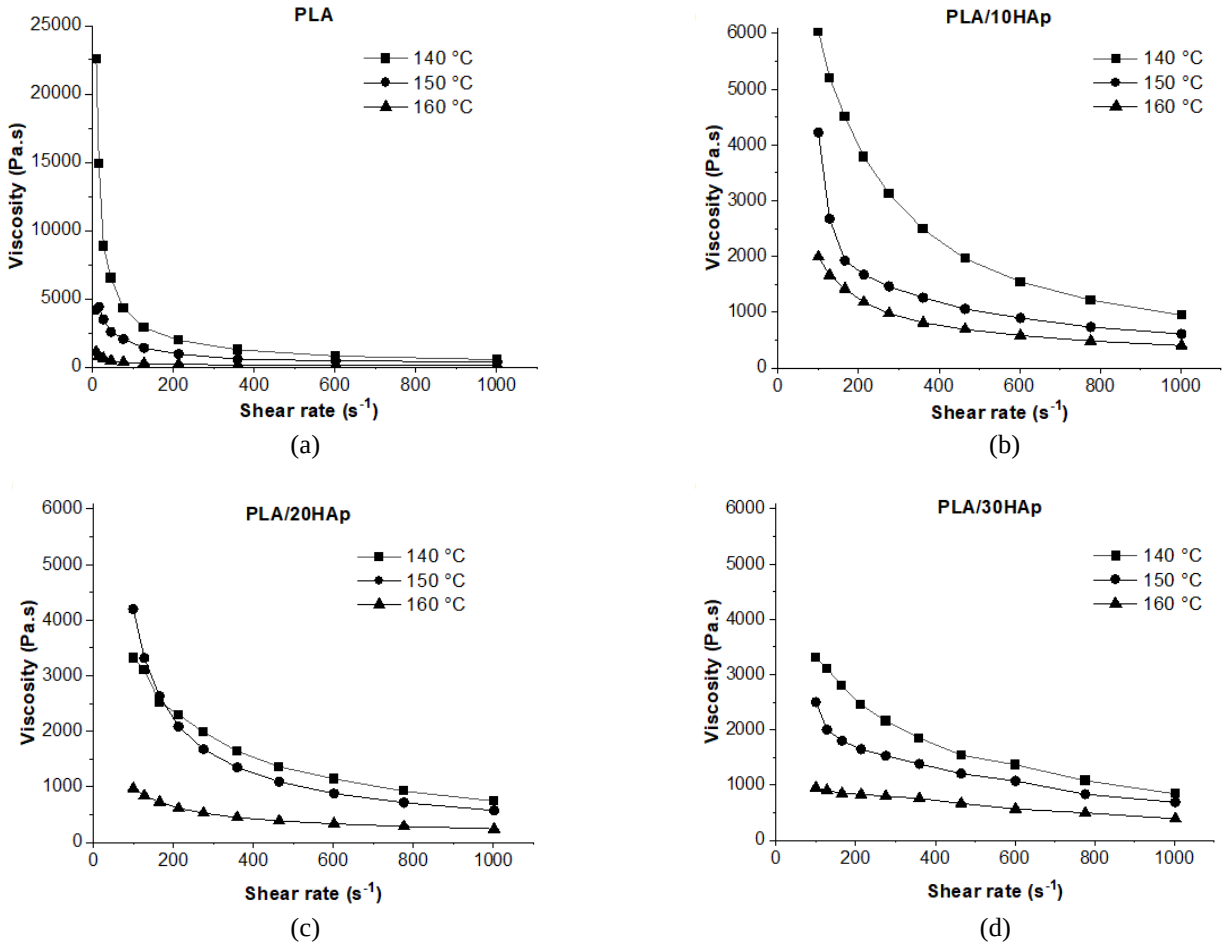

Figure 5. Viscosity vs shear rate of HAp/PLA composite at three different temperatures, (a) PLA, (b) PLA/10HAp, (c) PLA/20HAp and (d) PLA/30HAp

Based on the result, the graph of viscosity vs shear rate shows the viscosity baseline decreases when the HAp content increases in all the shear rate ranges analyzed. This data trend can be proved by referring to Figure 5 where at the temperature of 140 °C, the viscosity for PLA was 22600 Pa.s and had dropped to 6050, 3320 and 3300 Pa.s for PLA/10HAp, PLA/20HAp and PLA/30HAp, respectively as soon as the addition of ceramic filler. This is in agreement with previous research where the addition of 5 and 10 wt% of HAp had caused a decrease in viscosity [22]. The same data trend also can be observed at a temperature of 150 °C and 160 °C. This behavior indicates that the HAp has reduced the PLA thermodegradation activation energy and calcium has assisted in generating nucleophilic substitution processes [22]. According to Ignjatovic & Uskokovic [28], the HAp functional group, hydroxyl (OH-) has enhanced the composites' deterioration at high temperatures, hence the viscosity of the composites was observed to be decreased.

According to the graph, the HAp/PLA composite had a viscosity range of 10^2 to 10^4 Pa.s and a shear rate of 100 to 1000 s^{-1}. In 3D printing, lower viscosity is needed as the force of the flow will be minor to obtain a high printing quality [7]. Bragaglia et al. [6] show that the recommended range of viscosity for FDM 3D printing is between 10^2 and 10^5 Pa.s. The result indicates that the HAp/PLA composite has a viscosity of less than 10^4 Pa. For this reason, all feedstocks can be used to produce a newly developed composite filament to build objects using FDM printing. However, the optimum composition of HAp/PLA needs to be determined in order to proceed with the filament fabrication by evaluating the flow behavior index, *n* and activation energy, *E*.

Table 4 shows the flow behavior index, *n* for the HAp/PLA feedstock at three different temperatures, 140, 150 and 160 °C. The *n* value indicates the degree of viscosity sensitivity towards shear rate and temperature. According to the results, the *n* values for all temperatures were less than one ($n<1$), comparable to pseudoplastic flow, where this behavior refers to a reduction in viscosity as the shear rate increases, which is recommended in FDM 3D printing [7]. The *n* can be computed by applying the Power-Law equation as defined in Equation (2) where η is viscosity, *K* is consistency index, γ is shear rate and *n* is the power-law exponent (flow behaviour index).

$$\eta = K\,\gamma^{n-1} \tag{2}$$

Based on the observation of extruded feedstock flow quality, the feedstock at 160 °C presented a good consistency of viscosity, especially for compositions of 10 wt% and 20 wt% of HAp as the extrusion process is more stable and controllable with a continuous flow of the HAp/PLA mixed. It can be supported by the small differences of *n* values between 10 wt% and 20 wt% which are 0.308 and 0.396 respectively while for the 30 wt% the value is 0.647 which is much higher. This is because the concentration of PLA binder decreases which results in high viscosity and pores formation in the HAp/PLA mixture as shown in Figure 7(c). This flow defect like pores could affect the composite response toward the mechanical behavior [29]. Besides, most of the feedstock compositions have the lowest value of *n* at 140 °C, which could result in powder-binder separation that leads to inhomogeneities in printed samples. Hence, greater *n* values are generally chosen for solid-binder mixtures since they could minimize segregation issues [30].

Table 4. Flow Behavior Index, *n* obtained for HAp/PLA feedstocks

Feedstock Compositions	Temperature (°C)	Flow Behavior Index, *n*
PLA	140	0.197
	150	0.407
	160	0.436
PLA/10HAp	140	0.187
	150	0.248
	160	0.308
PLA/20HAp	140	0.347
	150	0.143
	160	0.396
PLA/30HAp	140	0.413
	150	0.495
	160	0.647

Another important property in evaluating the rheological behavior of feedstock is the flow activation energy, *E*. During the process of filament extruding, the temperature affects the *E* value of the HAp/PLA composite, which can be simplified using the Arrhenius equation, as demonstrated in Equation (3), where η is the viscosity of the mixture, ηo is the viscosity at a particular temperature, *E* is the flow activation energy, *R* is the universal gas constant and *T* is the temperature (Kelvin).

$$\eta = \eta o \exp(E/RT) \tag{3}$$

The trend line of the shear viscosity against reciprocal absolute temperature *(1/T)* for different feedstock compositions is demonstrated in Figure 6. The shear viscosity dependence on *1/T* in the temperatures 140 °C to 160 °C was observed to follow the Arrhenius equation, hence the value of *E* for all feedstocks was calculated from the slope of the trend line and the result was tabulated in Table 5. Based on the result, the *E* value for the viscous flow of pure PLA was determined to be 339 kJ/mol. The decrease in activation energy after the addition of HAp shows that this ceramic filler had enhanced polymer chain movement in a pseudo-Newtonian zone [31]. Research in 2021 shows that the *E* values for 10, 20 and 30 wt% of HAp for PCL/HAp composites were 2.24, 2.56 and 3.4 kJ/mol, respectively [32]. The *E* values evaluated in this previous study showed an opposite trend to the current study. In this case, the difference may be caused by the consequence of the polymer melt's pseudoplastic behavior during extrusion where HAp material had a direct role in decreasing the viscosity in the molten flow.

Table 5. Flow Activation Energy, *E* for HAp/PLA feedstocks

Feedstock Compositions	Flow Activation Energy, *E* (kJ/mol)
PLA	338.99
PLA/10HAp	68.85
PLA/20HAp	89.03
PLA/30HAp	53.62

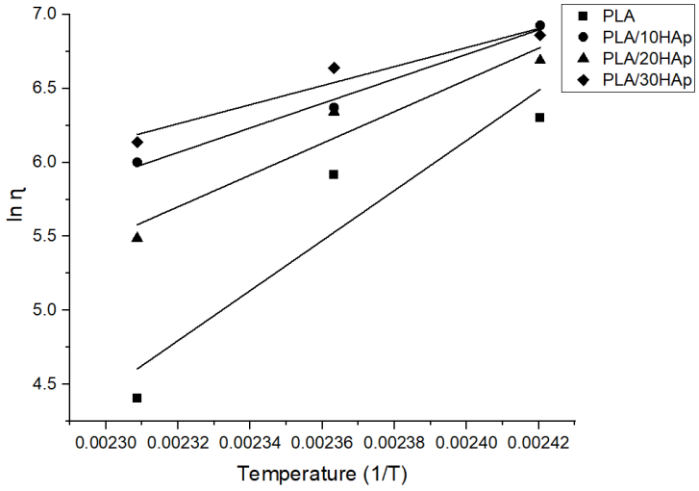

Figure 6. Viscosity vs temperature for HAp/PLA feedstock

Based on the evaluation of rheological behaviors for HAp/PLA feedstocks, the results demonstrated that the optimum composition is PLA/20HAp. This statement can be supported by referring to the *n* values at 160 °C (good fluidity) as depicted in Table 4. Too high *n* value like PLA/30HAp could lead to several problems as mentioned before, while too small *n* value like PLA/10HAp indicates that the feedstock is more sensitive towards the shear rates. This kind of scenario is undesirable since the feedstock has a higher viscosity dependence on the shear rate [33]. Hence, the *n* value like PLA/20HAp can be considered the best if compared with the others. In terms of *E*, a low value is required in 3D printing which corresponds to PLA/30HAp but if referred to the *n* values and extruded feedstock morphology, this composition is unsuitable to choose as optimum. Therefore, the optimum one is PLA/20HAp although the *E* value for this composition is high, it has the best *n* value, which is critical during the entire 3D printing process as the *E* value can still be minimized and controlled by optimizing the 3D printing parameters [34]. The higher E value signifies a greater energy required for flow compared to other compositions. In the context of DSC, this could be attributed to the existence of crystalline areas in the material that display greater stiffness, resulting in potential obstacles in the process of 3D printing. Nevertheless, the existence of crystallinity might occasionally reduce the material's tendency to flow and deform, which can be advantageous for specific 3D printing uses that require dimensional stability and mechanical strength. In such instances, the material's ability to retain its original structure and withstand warping can be advantageous. Therefore, the printing conditions for PLA/20HAp, which has been determined as the optimal option, can be adjusted to operate at temperatures higher than the T_c, where the material is in a more molten state. This facilitates enhanced extrusion and flow [35].

3.5 Morphological Analysis

Figure 7 shows the microstructure of extruded feedstock for HAp/PLA composite during the rheological testing at a temperature of 160 °C. Based on the SEM image of all compositions, the presence of bright particles which represent HAp was uniformly distributed throughout the PLA matrix. It was observed that flow defects such as voids (pores) and

numerous HAp agglomerations were noticed in some areas of the extruded feedstock, especially at PLA/30HAp. This shows that the more HAp content is added, the more crowded the particles will be, yielding to the rougher surface of the filament. This proved that HAp with more weightage content will affect the printing accuracy because of HAp's high brittleness which will lead to instabilities during the materials flow into the extruder. Therefore, the optimum composition to proceed with the fabrication of the filaments was determined to be PLA/20HAp as flow defects such as pores had occurred in the PLA/30HAp region. This kind of defect will cause stress concentration around the void area which easier for the crack to initiate and lastly, could affect the mechanical properties [29].

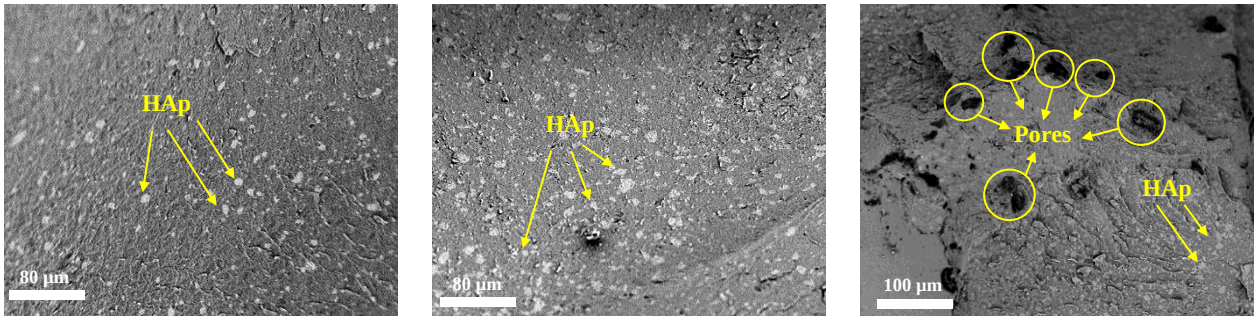

(a) (b) (c)

Figure 7. SEM image of extruded feedstock (a) PLA/10HAp (b) PLA/20HAp and (c) PLA/30HAp

4.0 CONCLUSION

In conclusion, an initial study of rheology for newly developed materials of HAp/PLA composite in producing the 3D printing filament was successfully evaluated. All HAp/PLA feedstocks produced by the extrusion process from the capillary rheometer demonstrated pseudoplastic flow which is favorable in 3D printing. However, based on the observation of extruded feedstock flow quality at 160 °C (good fluidity), rheological behavior and morphological structure, PLA/20 HAp is chosen as the optimum composition because this composition displayed a good flowability behavior with *n* and *E* values of 0.396 and 89.03 kJ/mol, respectively. Choosing a much higher content of HAp will be more complex in extruding and printing out the sample, hence PLA/20HAp is the best among others.

5.0 ACKNOWLEDGEMENT

The authors express their gratitude to the Ministry of Education and MYTRIBOS Industrial Grant (MIG) for providing financial support under Grant No. MIG-0015 as well as the College of Engineering, Universiti Teknologi MARA (UiTM) Shah Alam for provision of laboratory facilities.

6.0 REFERENCES

[1] M. N. M. Norani, M. I. H. C. Abdullah, M. F. Bin Abdollah, H. Amiruddin, F. R. Ramli, and N. Tamaldin, "Mechanical and tribological properties of FFF 3D-printed polymers: A brief review," *Jurnal Tribologi*, vol. 29, pp. 11–30, 2021.

[2] Y. A. Jin, H. Li, Y. He, and J. Z. Fu, "Quantitative analysis of surface profile in fused deposition modelling," *Additive Manufacturing*, vol. 8, pp. 142–148, 2015.

[3] R. M. German and A. Bose, *Injection molding of metals and ceramics*, Metal Powder Industries Federation, 1997.

[4] M. E. Mackay, "The importance of rheological behavior in the additive manufacturing technique material extrusion," *Journal of Rheology*, vol. 62, no. 6, pp. 1549–1561, 2018.

[5] A. Paar, "Tribology and rheology: Everything running smoothly?" Application Report, 2022. https://www.anton-paar.com/corp-en/services-support/document-finder/application-reports/joe-flow-tribology-and-rheology-everything-running-smoothly/ (accessed Apr. 18, 2022).

[6] M. Bragaglia, F.R. Lamastra, P. Russo *et al.*, "A comparison of thermally conductive polyamide 6-boron nitride composites produced via additive layer manufacturing and compression molding," *Polymer Composites*, vol. 42, no. 6, pp. 2751–2765, 2021.

[7] E. H. Backes, L. D. N. Pires, C. A. G. Beatrice, L. C. Costa, F. R. Passador, and L. A. Pessan, "Fabrication of biocompatible composites of poly(lactic acid)/hydroxyapatite envisioning medical applications," *Polymer Engineering and Science*, vol. 60, no. 3, pp. 636–644, 2020.

[8] D. Shekhawat, A. Singh, A. Bhardwaj, and A. Patnaik, "A short review on polymer, metal and ceramic based implant materials," *IOP Conference Series: Materials Science and Engineering*, vol. 1017, no. 1, p. 0120238, 2021.

[9] K. Choi, J. L. Kuhn, M. J. Ciarelli, and S. A. Goldstein, "The elastic moduli of human subchondral trabecular and cortical bone tissue," *Journal of Biomechanics*, vol. 23, no. 11, pp. 1103–1113, 1990.

[10] S. Liu, S. Qin, M. He, D. Zhou, Q. Qin, and H. Wang, "Current applications of poly(lactic acid) composites in tissue engineering and drug delivery," *Composites Part B: Engineering*, vol. 199, p. 108238, 2020.

[11] F. S. Senatov, K. V. Niaza, M. Y. Zadorozhnyy, A. V. Maksimkin, S. D. Kaloshkin, and Y. Z. Estrin, "Mechanical properties and shape memory effect of 3D-printed PLA-based porous scaffolds," *Journal of the Mechanical Behavior of Biomedical Materials*, vol. 57, pp. 139–148, 2016.

[12] C. Esposito Corcione, F. Scalera, F. Gervaso, F. Montagna, A. Sannino, and A. Maffezzoli, "One-step solvent-free process for the fabrication of high loaded PLA/HA composite filament for 3D printing," *Journal of Thermal Analysis and Calorimetry*, vol. 134, no. 1, pp. 575–582, 2018.

[13] R. N. Zare, E. Doustkhah, and M. H. N. Assadi, "Three-dimensional bone printing using hydroxyapatite-PLA composite," *Materials Today: Proceedings*, vol. 42, pp. 1531–1533, 2019.

[14] W. Wang, B. Zhang, M. Li, J. Li, C. Zhang, Y. Han, L. Wang, K. Wang, C. Zhou, L. Liu, and Y. Fan, "3D printing of PLA/n-HA composite scaffolds with customized mechanical properties and biological functions for bone tissue engineering," *Composites Part B: Engineering*, vol. 224, p. 109192, 2021.

[15] F. S. Senatov, K. V. Niaza, A. A. Stepashkin, and S. D. Kaloshkin, "Low-cycle fatigue behavior of 3d-printed PLA-based porous scaffolds," *Composites Part B: Engineering*, vol. 97, pp. 193–200, 2016.

[16] F.S. Senatov, M.Y. Zadorozhnyy, K.V. Niaza, V. Medvedev, S.D. Kaloshkin, N.Y. Anisimova, M.V. Kiselevskiy, and K.C. Yang, "Shape memory effect in 3D-printed scaffolds for self-fitting implants," *European Polymer Journal*, vol. 93, pp. 222–231, 2017.

[17] A. P. Marzuki, F. M. Salleh, M. N. S. Rosli, I. Tharazi, A. H. Abdullah, and N. H. A. Halim, "Rheological, mechanical and physical properties of Poly-Lactic Acid (PLA)/ Hydroxyapatites (HA) composites prepared by an injection moulding process," *Journal of Mechanical Engineering*, vol. 19, no. 2, pp. 17–39, 2022.

[18] S. Esmaeili, H. Aghdam, M. Motififard, S. Saber-Samandari, A.H. Montazeran, M. Bigonah, E. Sheikhbahaei, and A. Khandan, "A porous polymeric–hydroxyapatite scaffold used for femur fractures treatment: fabrication, analysis, and simulation," *European Journal of Orthopaedic Surgery and Traumatology*, vol. 30, no. 1, pp. 123–131, 2020.

[19] V. Hughes, I. Tabiai, K. Chizari, and D. Therriault, "3D Printable Conductive Nanocomposites of PLA and Multi-Walled Carbon Nanotubes," École Polytechnique Montréal, Canada, Technical Report, no. 11.2, 2016.

[20] F. Chinellato, J. Wilbig, D. Al-Sabbagh, P. Colombo, and J. Günster, "Gas flow assisted powder deposition for enhanced flowability of fine powders: 3D printing of α-tricalcium phosphate," *Open Ceramics*, vol. 1, pp. 4–11, 2020.

[21] P. Singh, V. K.Balla, S. V.Atre, R. M.German, and K. H.Kate, "Factors affecting properties of Ti-6Al-4V alloy additive manufactured by metal fused filament fabrication," *Powder Technology*, vol. 386, pp. 9–19, 2021.

[22] E. H. Backes, E. M. Fernandes, G. S. Diogo, C. F. Marques, T.H. Silva, L.C. Costa, F.R. Passador, R.L. Reis, and L.A. Pessan, "Engineering 3D printed bioactive composite scaffolds based on the combination of aliphatic polyester and calcium phosphates for bone tissue regeneration," *Materials Science and Engineering: C*, vol. 122, p. 111928, 2021.

[23] M. Raimo, "Impact of thermal properties on crystalline structure, polymorphism and morphology of polymer matrices in composites," *Materials*, vol. 14, no. 9, p. 2136, 2021.

[24] C. Yang, X. Tian, D. Li, Y. Cao, F. Zhao, and C. Shi, "Influence of thermal processing conditions in 3D printing on the crystallinity and mechanical properties of PEEK material," *Journal of Materials Processing Technology*, vol. 248, pp. 1–7, 2017.

[25] B. Van de Voorde, A. Katalagarianakis, S. Huysman, A. Toncheva, J.M. Raquez, I. Duretek, C. Holzer, L. Cardon, K.V. Bernaerts, D. Van Hemelrijck, and L. Pyl, "Effect of extrusion and fused filament fabrication processing parameters of recycled poly(ethylene terephthalate) on the crystallinity and mechanical properties," *Additive Manufacturing*, vol. 50, p. 102518, 2022.

[26] S. Liu, Y. Zheng, R. Liu, and C. Tian, "Preparation and characterization of a novel polylactic acid/hydroxyapatite composite scaffold with biomimetic micro-nanofibrous porous structure," *Journal of Materials Science: Materials in Medicine*, vol. 31, no. 8, 2020.

[27] E. E. Popa, M. Rapa, O. Popa, G. Mustatea, V.I. Popa, A.C. Mitelut, and M.E. Popa, "Polylactic acid/cellulose fibres based composites for food packaging applications," *Materiale Plastice*, vol. 54, no. 4, pp. 673–677, 2017.

[28] N. Ignjatovic and D. Uskokovic, "Synthesis and application of hydroxyapatite / polylactide composite biomaterial," *Applied Surface Science*, vol. 238, pp. 314–319, 2004.

[29] M. Mehdikhani, L. Gorbatikh, I. Verpoest, and S. V. Lomov, "Voids in fiber-reinforced polymer composites: A review on their formation, characteristics, and effects on mechanical performance," *Journal of Composite Materials*, vol. 53, no. 12, pp. 1579–1669, 2019.

[30] M. Strano, K. Rane, F. Briatico Vangosa, and L. Di Landro, "Extrusion of metal powder-polymer mixtures: Melt rheology and process stability," *Journal of Materials Processing Technology*, vol. 273, p. 116250, 2019.

[31] G. Luiz, Ecco, S. Dul, D.P. Schmitz, G.M. Barra, B.G. Soares, L. Fambri, and A. Pegoretti, "Rapid prototyping of efficient electromagnetic interference shielding polymer composites via fused deposition modeling," *Applied Sciences (Switzerland)*, vol. 9, no. 1, p. 37, 2018.

[32] Z. Laja Besar, S. Akhbar, S. Alam, and S. Darul Ehsan, "Effect of particle size, shape, and weight percentage of hydroxyapatite (HA) on rheological behaviour of polycaprolactone/hydroxyapatite (PCL/HA) composites," *Malaysian Journal of Chemical Engineering & Technology Journal Homepage*, vol. 4, no. 2, pp. 132–136, 2021.

[33] S. Y. M. Amin, K. R. Jamaludin, and N. Muhamad, "Rheological properties of Ss316L Mim feedstock prepared with different particle sizes and powder loadings," *The Institution of Engineers, Malaysia*, vol. 71, no. 2, pp. 59–63, 2009.

[34] M. Y. Zakaria, A. B. Sulong, M. I. Ramli, B. Ukwueze, W. S. W. Harun, and R. L. Mahmud, "Fabrication of porous titanium-hydroxyapatite composite via powder metallurgy with space holder method," *Journal of Advanced Manufacturing Technology*, vol. 12, no. 1, pp. 37–48, 2018.

[35] D. Vaes and P. Van Puyvelde, "Semi-crystalline feedstock for filament-based 3D printing of polymers," *Progress in Polymer Science*, vol. 118, pp. 1–42, 2021.